Electronic Supplementary Material (ESI) for Soft Matter.

Weak Polyelectrolyte Brushes: Re-entrant Swelling and Self-Organization

Vincent Senechal,[1,2] Hassan Saadaoui,[1,2] Nelson Vargas-Alfredo[3], Juan Rodriguez-Hernandez[3] and Carlos Drummond[1,2,]
1 CNRS, Centre de Recherche Paul Pascal (CRPP), UMR 5031, F-33600 Pessac, France
2 Université de Bordeaux, Centre de Recherche Paul Pascal. F- 33600 Pessac, France
3 Instituto de Ciencia y Tecnología de Polímeros, CSIC, Juan de la Cierva 3, 28006, Madrid, Spain

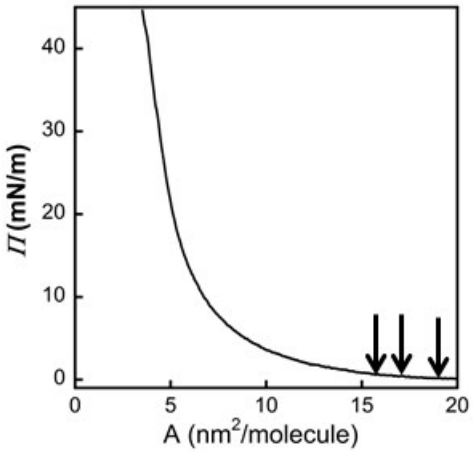

Figure S1.a) Compression isotherm of the PS_{36}-*b*-PAA_{125} monolayer at the air-water interface. The arrows indicate the compression condition for the different polymer layers studied in this work

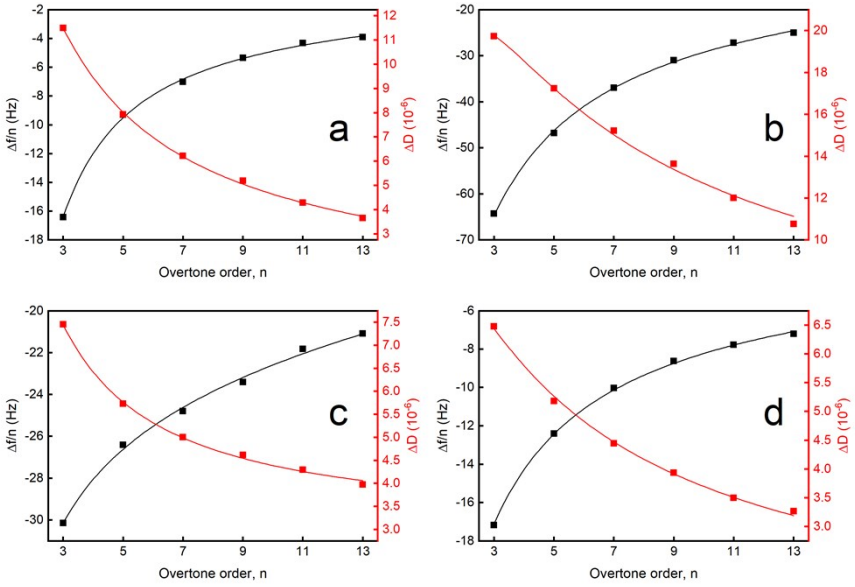

Figure S2. Some examples of QCM-D data fit, using the small load approximation. Symbols correspond to the experimental Δf and ΔD data; the lines are the result of the fit of data, as explained in the main text. a) 0.07 chains/nm^2, pH 6. b) 0.0 7 chains/nm^2, pH 10; c) 0.05 chains/nm^2, pH 8; d) 0.05 chains/nm^2, pH4, [KCl] 50mM

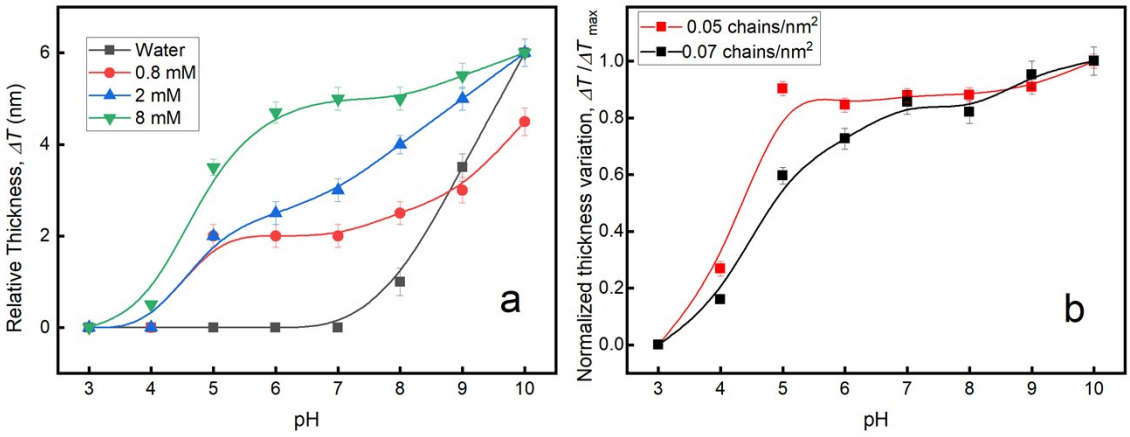

Figure S3. a) Thickness variation of a self-assembled film of $(PAA_{47})_2S_2$ as a function of pH, calculated from changes in Δf and ΔD of the coated quartz crystal, as described in the main text. The concentration of the indifferent electrolyte (KCl) is indicated in the legend. The non-monotonic evolution of thickness with pH at low and intermediate salt concentration can be observed. b) Relative thickness variation of PS_{36}-*b*-PAA_{125} films vs pH, calculated from changes in Δf and ΔD of the coated quartz crystal, as described in the text [KCl]=2mM. PS_{36}-*b*-PAA_{125} density indicated in the legend.

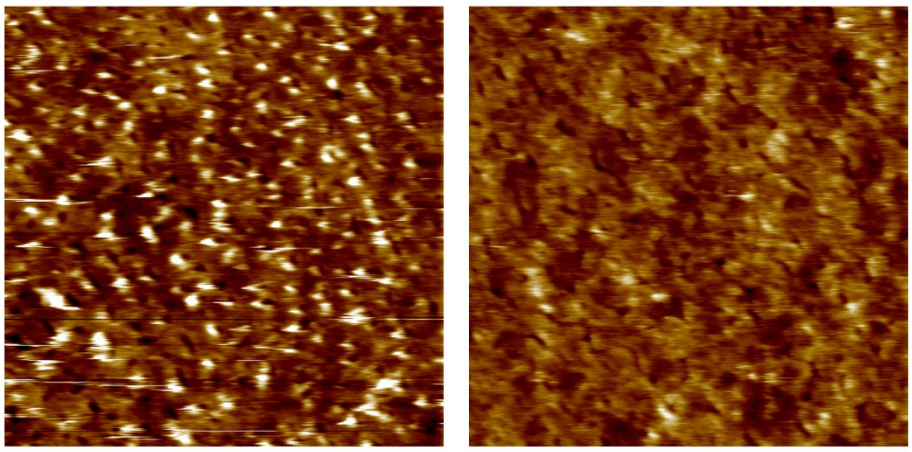

Figure S4. 1µm x 1µm soft-contact mode height AFM micrograph of a PS_{36}-*b*-PAA_{125} film measured in water, pH=7. Film transferred at surface pressure Π=0.2 mN/m (0.05 chains/nm^2). Left: No salt added. The heterogeneous aspect of the polymer brush can be clearly observed in this condition of low ionic strength. Right: [KCl]=8mM. The intrachain electrostatic repulsion is greatly screened, and the polymer layer becomes homogeneous

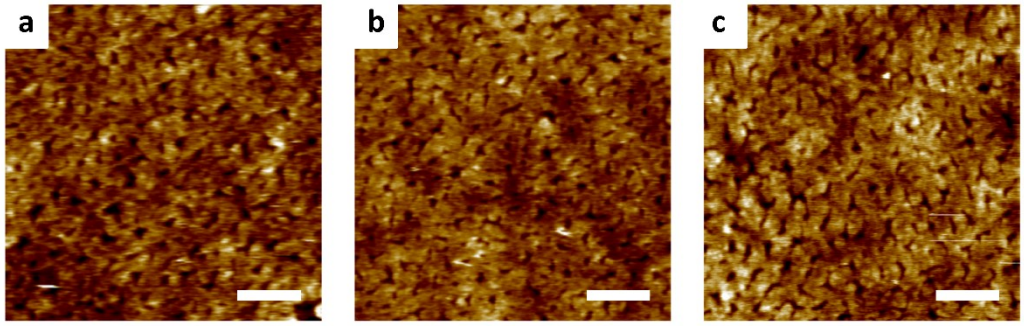

Figure S5. Soft-contact mode height AFM micrograph of a PS_{36}-*b*-PAA_{125} film measured in water, pH=5. 0.07 chains/nm^2. [KCl]=8 mM a) pH=3. b) pH=7. c) pH=10 (scale bars 200 nm)

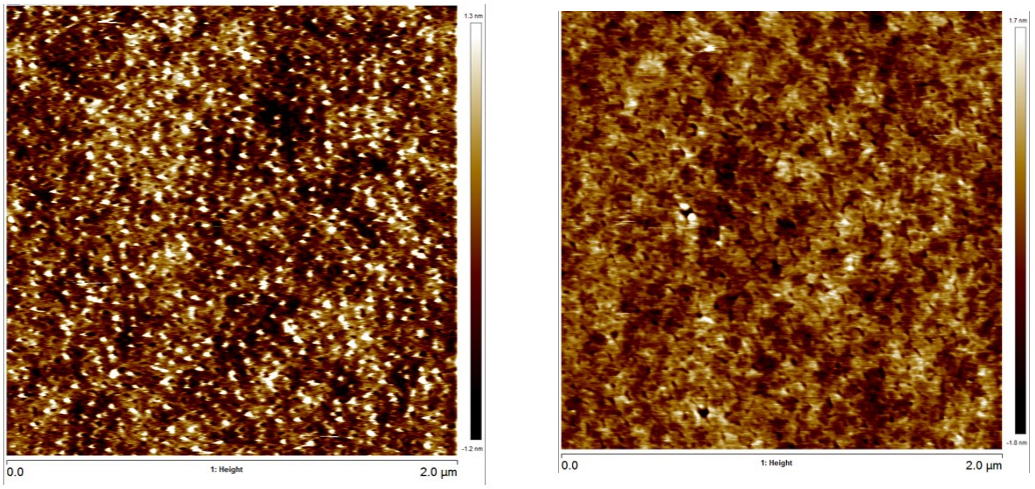

Figure S6. Soft-contact mode height AFM micrograph of a PS_{36}-*b*-PAA_{125} film measured in water, pH=5. Film transferred at surface pressure Π=0.2 mN/m (0.05 chains/nm^2). Left: pH 5. The heterogeneous aspect of the polymer brush can be clearly observed in this condition of low ionic strength. Right: pH 10. Polymer chains become fully charge, and the polymer layer becomes homogeneous

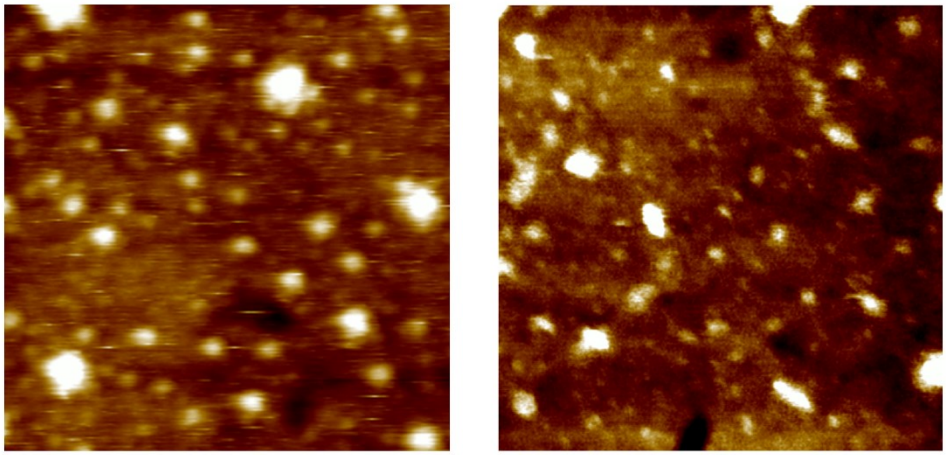

Figure S7. 500 nm x 500 nm peak-force mode height AFM micrographs of a $(PAA_{47})_2S_2$ self-assembled film measured in water (pH 6)

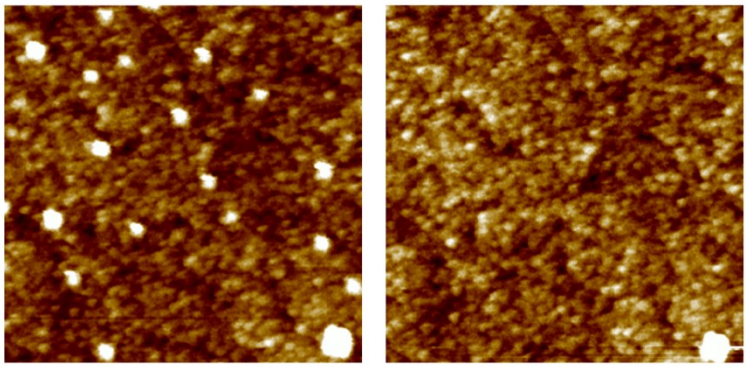

Figure S8. 400 nm x 400 nm peak-force mode height AFM micrograph of a $(PAA_{47})_2S_2$ self-assembled film measured in water, pH=5.9. The maximum applied force (set point) was fixed to the minimum value for which a stable image could be obtained (ca. 150 pN). The two images were measured in the same area on the surface. In the second scan (right) higher features observed in the first scan (left) disappeared.

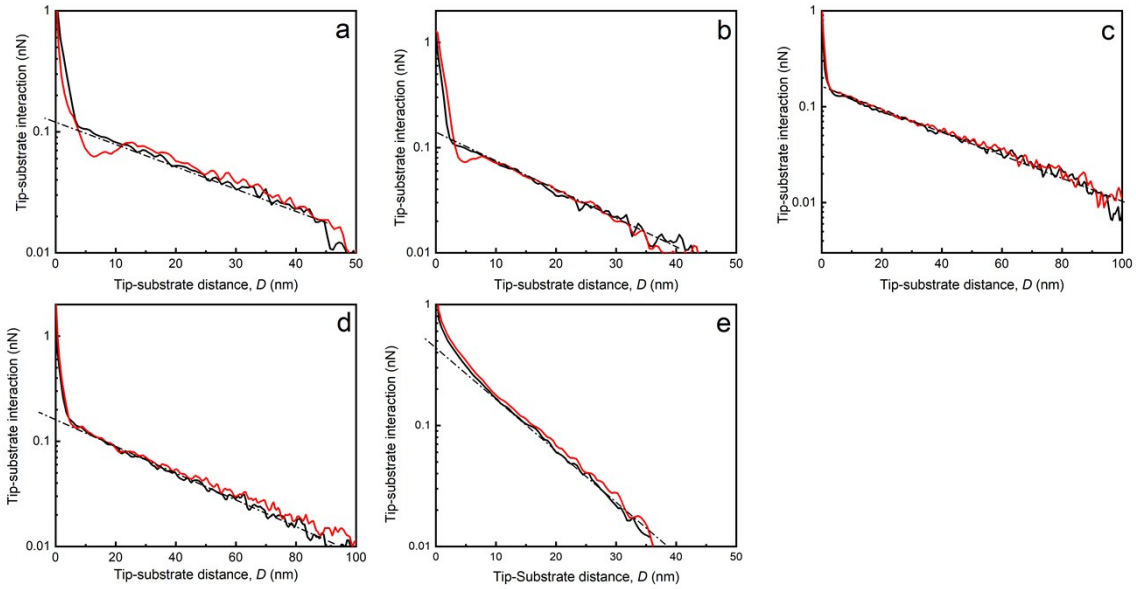

Figure S9. Normal Interaction force between the AFM silicon tip and the self-assembled film of $(PAA_{47})_2S_2$ measured on approach (black lines) and separation (red lines) at pH (a) 5.1, (b) 6.2, (c) 7.2, (d) 8.7, and (e) 11.3. The dash-dotted lines on each graph correspond to a single exponential fit of the measured force at large separations.

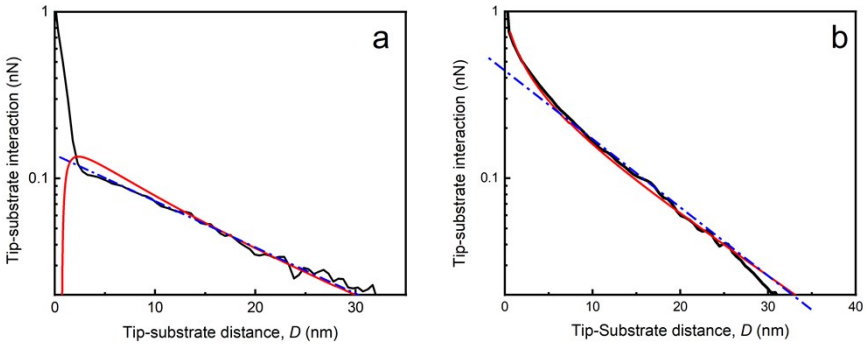

Figure S10. Normal Interaction force between the AFM silicon tip and the self-assembled film of $(PAA_{47})_2S_2$ measured on approach (black lines) at pH (a) 6.2, and (b) 11.3. The dash-dotted blue line on each graph correspond to a single exponential fit of the measured force at large separations. The red curves are calculated by fitting the data at large separations (15 nm< D <30 nm) and using the results to extrapolate to the complete distance range by numerical integration of the full Poisson-Boltzmann equation, considering constant potential (pH 6.2) and constant charge (pH 11.3) boundary conditions, and Hamaker constant 5.10^{-20} J.

Table S1. Characteristic decay length of the measured tip-substrate interaction force, and expected Debye length λ considering the ionic strength is determined by the exclusive presence of H_3O^+ and OH^- ions at different pH

pH	Measured decay length (nm)	λ (nm)
8	37.3	304
10	30.2	30.4
11	9.7	9.61